

## WAVE PATTERN PREDICTION OF MONOHULLS AND CATAMARANS IN A SHALLOW-WATER CANAL BY LINEARISED THEORY

Mustafa İNSEL\* and Lawrence J. DOCTORS

Australian Maritime Engineering Cooperative Research Centre  
Sydney Node, The University of New South Wales,  
Sydney, NSW,  
AUSTRALIA

### ABSTRACT

The prediction of the far-field wave pattern of a ship in shallow water canal is important to assess the wash on the river banks. In this paper, an approach based on linear theory is presented. A series of wave-pattern surveys have been conducted for a series of mathematically defined hull forms. The wave spectrum predictions are compared with experimental measurements in deep and shallow water. A method for the prediction of catamaran wave patterns is derived and compared with the experimental measurements.

### INTRODUCTION

Prediction of wave resistance of a surface ship by linearised theory has been utilised satisfactorily for slender hull forms (Doctors et al 1991, Insel et al 1994). Linearised theory can also be used for the prediction of the far-field wave pattern, or so called wave wake, behind the hull. The prediction of the wave pattern is particularly important in a shallow water canal or river in order to assess river bank erosion.

Linearised theory of ship waves and ship wave resistance has been developed since Michell (1898) formulated deep-water wave resistance. Shallow water and canal wall effects were investigated by Strettensky (1936) and Lunde (1951). In this paper, an approach based on linear theory is used to determine the far-field wave coefficients of a hull or a multihull as well as the wave resistance.

Eggers (1962) has outlined an approach to measure the far-field wave pattern of a hull by using a Fourier analysis. Experimental work has been carried out by using this analysis technique on a mathematically defined hull form series in order to assess the adequacy of the calculated wavemaking in the current work.

### FAR-FIELD WAVE SYSTEM IN SHALLOW CANAL

Assuming the fluid is ideal and incompressible, the flow is steady and irrotational, the linearised boundary conditions can be expressed in a Cartesian axis system shown in Figure 1 :

#### i) Laplace equation

$$\nabla^2 \phi = \frac{\partial^2 \phi}{\partial x^2} + \frac{\partial^2 \phi}{\partial y^2} + \frac{\partial^2 \phi}{\partial z^2} = 0 \quad (1)$$

#### ii) Free surface conditions

##### a) Dynamic free surface condition

$$g\zeta + U\phi_x = 0 \quad \text{at } z=0 \quad (2)$$

##### b) Kinematic free surface condition

$$U\zeta_x - \phi_z = 0 \quad \text{at } z=0 \quad (3)$$

#### iii) Bottom condition

$$\phi_z = 0 \quad \text{at } z=-H \quad (4)$$

#### iv) Radiation condition

$$\lim_{(x^2+y^2) \rightarrow \infty} \phi = \begin{cases} \alpha(1) & \text{for } x < 0 \\ 0 & \text{for } x > 0 \end{cases} \quad (5)$$

#### v) Hull surface condition

$$Uf_x + \phi_y = 0 \quad \text{at } y=f(x,z) \quad (6)$$

where the free surface is expressed as  $z=\zeta(x,y)$  and geometry of the ship is represented by  $y=f(x,z)$ .

The velocity potential of a source with density of  $\mu_0$  and located at  $(x_0, y_0, z_0)$  in shallow water canal with a depth  $H$  and a width  $W$  (Figure 1) can be obtained by considering images due to the tank walls at  $y_0' = y_0 + 2mW$  and  $y_0'' = y_0 + (2m+1)W$  for  $m = -\infty, \infty$  of the source and its image due to the tank bottom at  $z' = -(2H+z_0)$ . The far field velocity potential of a source can then be found and is given by

\* Permanent Address : Faculty of Naval Architecture and Ocean Engineering, İstanbul Technical University, İstanbul, TURKEY

İnsel (1990) as;

$$\phi_{FF} = \frac{g}{U} \sum_{m=0}^{\infty} \left[ -\frac{\eta_m}{\beta_m} \cos(\omega_m x) + \frac{\xi_m}{\alpha_m} \sin(\omega_m x) \right] \frac{1}{K_m \cos \theta_m} \quad (7)$$

$$\frac{\cosh(K_m(z+H))}{\cosh(K_m H)} \frac{\cos(m\pi y/W)}{\sin(m\pi y/W)} \quad \begin{matrix} \text{for even } m \\ \text{for odd } m \end{matrix}$$

where

$$\xi_m = \int_S \mu_0 \tau_m \cos(m\pi y_0/W) \frac{\cos(\omega_m x_0)}{\sin(\omega_m x_0)} dx_0 dz_0 \quad \begin{matrix} \text{for even } m \\ \text{for odd } m \end{matrix} \quad (8)$$

$$\alpha_m = \int_S \mu_0 \tau_m \sin(m\pi y_0/W) \frac{\cos(\omega_m x_0)}{\sin(\omega_m x_0)} dx_0 dz_0 \quad \begin{matrix} \text{for even } m \\ \text{for odd } m \end{matrix} \quad (9)$$

$$\tau_m = \frac{16\pi U}{Wg} \frac{e^{-K_m H} \cosh(K_m(H+z_0))}{(1 - K_0 H \operatorname{sech}^2(K_m H) + \sin^2 \theta_m)} (K_0 + K_m \cos^2 \theta_m) \quad (10)$$

$$\omega_m = K_m \cos \theta_m \quad (11)$$

where  $K_m$  and  $\theta_m$  are solution of

$$K_m - K_0 \sec^2 \theta_m \tanh(K_m H) = 0 \text{ and } K_m \sin \theta_m = \pi m/W$$

The far field wave elevation can be found from dynamic free surface condition and is given by İnsel (1990) as;

$$\zeta = \sum_{m=0}^{\infty} \left[ \frac{\xi_m}{\alpha_m} \cos(\omega_m x) + \frac{\eta_m}{\beta_m} \sin(\omega_m x) \right] \frac{\cos(m\pi y/W)}{\sin(m\pi y/W)} \quad \begin{matrix} \text{for even } m \\ \text{for odd } m \end{matrix} \quad (12)$$

For practical calculations  $m$  can be truncated at a finite number  $M$ .  $\xi_m$  and  $\eta_m$  are the amplitudes of the symmetric wave components relative to the tank centerline, meanwhile  $\alpha_m$  and  $\beta_m$  are that of the asymmetric wave components. For a symmetric hull form relative to the canal centerline,  $\alpha_m$  and  $\beta_m$  are zero. Hence, by substituting  $m=2n$  and ( $M=2N$ ):

$$\zeta = \sum_{n=0}^N \left[ \xi_n \cos(\omega_n x) + \eta_n \sin(\omega_n x) \right] \cos(2n\pi y/W) \quad (13)$$

Thus the wave system of a source at the centerline of the canal, or a symmetric source distribution, can be represented by a finite number of discrete wave components with angle of  $\theta_n$ , wave number of  $K_n$ , wave frequency of  $\omega_n$  and amplitude of  $\zeta^2 = \xi^2 + \eta^2$  (Figure 2). The use of a finite number of wave components is justified as the harmonic number ( $n>20$ ) is increased the angle of wave reaches very high angles ( $\theta_n>70$ ).

Evaluation of wave coefficients is performed for a combination of source-sink distribution where source strength is derived from thin ship assumption over panels distributed on the centerplane of the hulls. The numerical code also includes routines to trim and increase/decrease draught of the hull form at any speed.

## WAVE RESISTANCE OF A SHIP MODEL IN A SHALLOW CANAL

The wave resistance can be obtained from considerations of energy changes as given by İnsel (1990):

$$R_w = \frac{W\rho g}{4} \left[ (\xi_0^2 + \eta_0^2) \left( 1 - \frac{2K_0 H}{\sinh(2K_0 H)} \right) + \sum_{m=1}^M \left[ \frac{\xi_m^2 + \eta_m^2}{\alpha_m^2 + \beta_m^2} \left[ 1 - \frac{\cos^2 \theta_m}{2} \left( 1 + \frac{2K_m H}{\sinh(2K_m H)} \right) \right] \right] \right] \quad (14)$$

$\xi_n, \eta_n$  and  $\alpha_n, \beta_n$  are amplitude of wave coefficients in wave resistance due to symmetric and asymmetric wave pattern respectively.

## FAR FIELD WAVE PATTERN OF A CATAMARAN

As a special case a catamaran made up two symmetrical demihulls is investigated as it is the main concern for practical applications. For such a craft, two hulls will be located at  $y_1 = -S/2$  and  $y_2 = S/2$  (İnsel 1994):

$$\zeta = \sum_{n=0}^N [2\xi_n C_s \cos(\omega_n x) + 2\eta_n C_s \sin(\omega_n x)] \cos\left(\frac{2n\pi y}{W}\right) \quad (15)$$

$$R_w = \frac{W\rho g}{4} \left[ ((2\xi_0)^2 + (2\eta_0)^2) \left( 1 - \frac{2K_0 H}{\sinh(2K_0 H)} \right) + \sum_{n=1}^N [(2\xi_n C_s)^2 + (2\eta_n C_s)^2] \left[ 1 - \frac{\cos^2 \theta_n}{2} \left( 1 + \frac{2K_n H}{\sinh(2K_n H)} \right) \right] \right] \quad (16)$$

where

$$C_s = \cos(K_n S/2 \sin \theta_n) = \cos(\pi n S/W) \quad (17)$$

It is also noted that catamaran wave coefficients can also be obtained by applying experimentally obtained values of  $\xi_n, \eta_n$  from the wave pattern analysis of a demihull.

## EXPERIMENTAL APPROACH

In order to assess the capabilities of the theoretical model, comparisons with the experiments must be made. The common comparison for the theoretical wave resistance calculation is to compare with the wave resistance ( $C_w = C_T - (1+k)C_F$ ). But such an approach does not include the effects of the wave spectrum.

Wave pattern analysis approach given by Eggers (1962) represents an effective approach to the analysis of the wave pattern. A method based on multiple longitudinal cuts (İnsel 1990) is adapted for the current experiments.

Two sets of experiments have been conducted. Firstly, total resistance and wave pattern experiments with a mathematically defined form (Figure 3), Wigley Hull, have been conducted both in free and fixed to trim-and-sinkage conditions. The wave resistance coefficient comparison is given in Figure 4 for the fixed condition. Linear theory generally overpredicts the wave resistance. To correct this feature, a correction method was considered (Doctors 1991, Doctors 1992). A second set of experiments was conducted by introducing a parallel middle body to the Wigley model. Length, beam, draught have been kept constant resulting in only  $C_p$ ,  $C_b$  and angle of entrance change. Both deep and shallow-water tests have been conducted.

## COMPARISON OF MEASURED AND CALCULATED WAVEMAKING

The wave amplitudes across the wave angle spectrum are given for two speeds for fixed hull in Figures 5 and 6. The prediction of linear theory is generally higher than the experimental wave coefficients for small wave angles, transverse wave system. A modification to the theoretical results is applied as a constant multiplier depending only on the Froude number by using a least-square regression technique. Although this correction fits well with low wave angles, predictions for higher angles become too low.

The wave-pattern system generated by the modified linear theory is demonstrated and compared with the experimental longitudinal wave traces in Figures 7 and 8. The phase of the predicted wave pattern is in agreement with experiments.

As the linear theory is based on fixed-to-trim-and-sinkage model, a comparison of theory and experiments for the



free condition is conducted by trimming and changing the draught of the input hull form into the theory. The results are given in Figure 9 for one Froude number. The results are in similar agreement to those for the fixed case.

Catamaran configurations of this hull have also been tested for separation-to-length ratios of 0.2 to 0.5. A comparison of predicted and measured catamaran wave amplitude is given in Figure 10. The predictions in this figure were based on experimental measurements of a demihull alone. The predictions up to wave angle of 50 degrees are in agreement with experiments, above this wave angle there are some discrepancies between theory and experiments.

The shallow water effects were investigated on a mathematically defined form. Figure 11 demonstrates the change of wave coefficients with change of water depth.

In practical design work, a comparative study of hull form variation is the main concern. Hence the second set of experiments have been utilised to demonstrate the sensitivity of the linear theory. The wave amplitude across the wave spectrum for one speed is given in Figure 12. Predictions display the same trends as the experiments. I.e. the decrease of wave amplitude at transverse waves (low angles) and increase of wave amplitude at divergent waves (high angles) with increasing  $C_p$  are predicted satisfactorily.

## CONCLUSIONS

Linearised theory can be used for the prediction of wave resistance of slender hull forms in shallow canal. The far-field wave pattern can also be predicted by this method. Although the predicted wave amplitude is higher than the experimental amplitude, the wave phase is in good agreement.

Effects of trim and sinkage can simply be taken into account by changing the trim and draught of hull form in the calculations.

Prediction of catamaran wave pattern from demihull wave pattern can be conducted satisfactorily.

The effect of hull form changes on the wave pattern can also be predicted satisfactorily.

Hence, linear theory presents a simple but efficient approach to predict the far field wave pattern of slender forms, even in shallow water and canal conditions.

## REFERENCES

- Doctors L.J., Renilson M.R., Parker G., Hornsby N., 1991, "Waves and Wave Resistance of a High Speed River Catamaran", *Proc. First International Conference on Fast Sea Transportation (FAST 91)*, Norwegian Institute of Technology, Trondheim, Norway, Vol:1, pp .35-52
- Doctors L.J., Renilson M.R., 1992, "Corrections for Finite Water-Depth Effects on Ship Resistance", *Proc. Eleventh Australasian Fluid Mechanics Conference (11 AFMC)*, University of Tasmania, Hobart, Tasmania, Australia, Vol:1, pp.663-666
- Eggers K.W.H., 1962, "Über die Ermittlung des Wellenwiderstandes eines Schiffmodells durch Analyse seines Wellensystems", *Schifftechnik*, Band 9, Heft 46
- Insel M., 1990, "An Investigation into the Resistance Components of High Speed Catamarans", Ph.D.Thesis, Department of Ship Science, Univ.of Southampton, UK
- Insel M., Molland A.F., Wellicome J.F., 1994, "Wave

Resistance Prediction of a Catamaran by linearised Theory", *CADMO 94*, Southampton UK

Lunde J.K., 1951, "On the Linearized Theory of Wave Resistance for Displacement Ships in Steady and Accelerated Motion", *Transactions of SNAME*, Vol:59, pp. 25-76

Michell J.H., 1898, "The Wave Resistance of a Ship", *Philosophical Magazine*, London, Series 5, Vol:45, pp. 106-123

Sretten L.N., 1936, "On the Wavemaking Resistance of a Ship Moving Along in a Canal", *Philosophical Magazine and Journal of Science*, Vol:22-Seventh Series, December

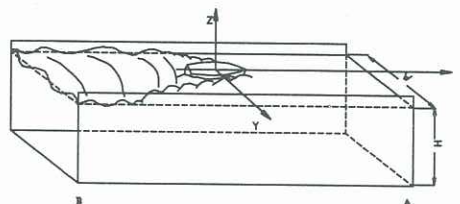


Figure 1: Axis System and Canal Dimensions

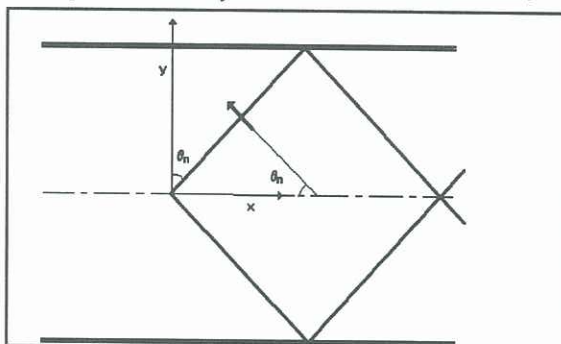


Figure 2: Angle and Direction of Wave Components

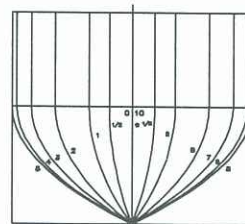


Figure 3: Mathematical Hull Form (Wigley Hull)

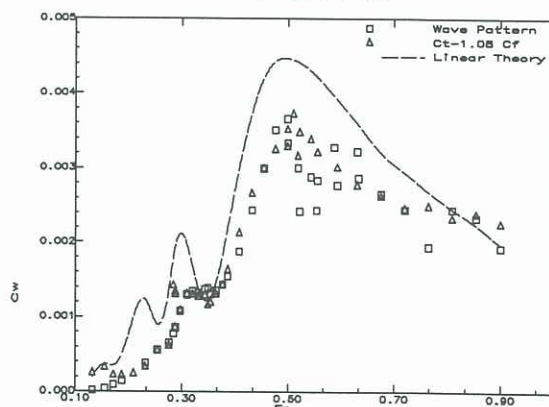


Figure 4: Wave Resistance of Mathematically Defined Hull Form

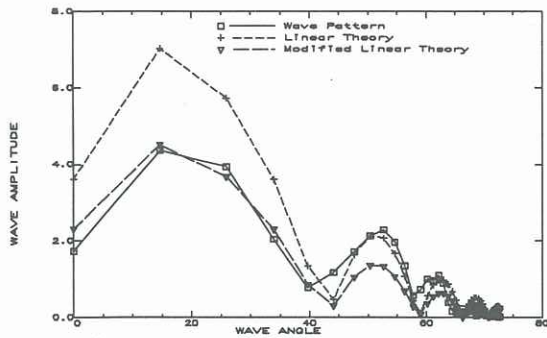


Figure 5: Wave Amplitude Across the Wave Angle Spectrum (Wigley Hull-Fixed to Trim and Sinkage,  $Fn:0.30$ )

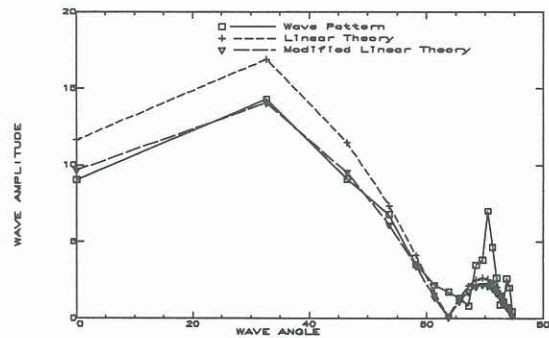


Figure 6: Wave Amplitude across the Wave Angle Spectrum (Wigley Hull-Fixed to Trim and Sinkage,  $Fn:0.50$ )

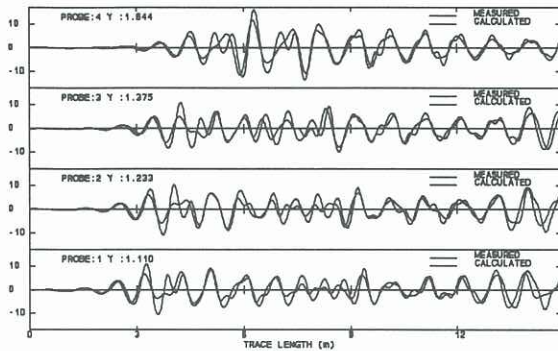


Figure 7: Measured and Calculated Wave Elevations (Wigley Hull-Fixed to Trim and Sinkage,  $Fn:0.30$ )

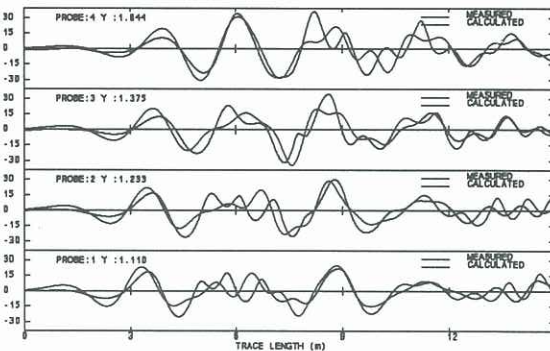


Figure 8: Calculated and Measured Wave Elevations (Wigley Hull-Fixed to Trim and Sinkage,  $Fn:0.50$ )

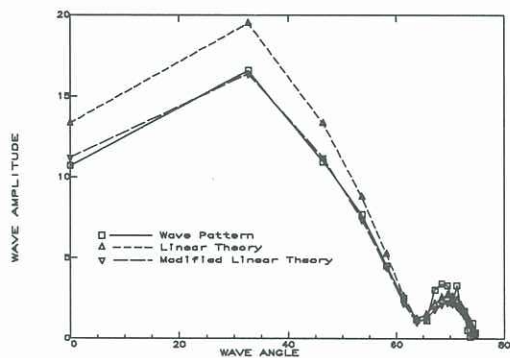


Figure 9: Wave Amplitude across the Wave Angle Spectrum (Wigley Hull-Free to Trim and Sinkage,  $Fn:0.50$ )

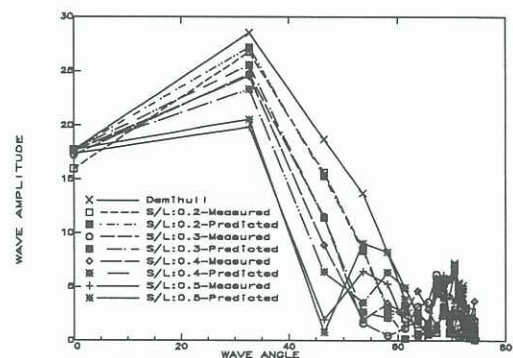


Figure 10: Wave Amplitude across the Wave Angle Spectrum (Wigley Hull Cat-Fixed to Trim and Sinkage,  $Fn:0.50$ )

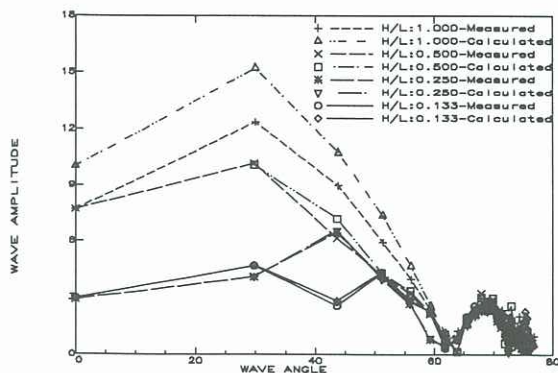


Figure 11: Wave Amplitude in Shallow Water ( $Fn:0.50$ )

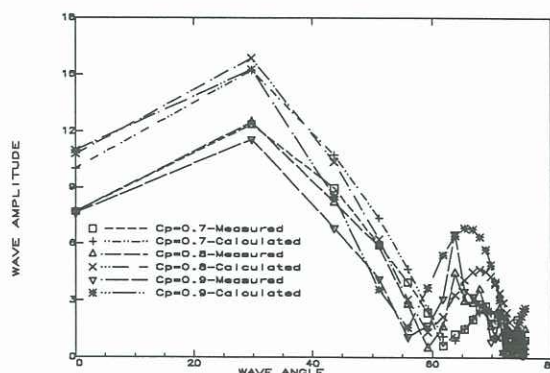


Figure 12: Wave Amplitude Change with Hull Fullness